Anharmonic oscillator representation of nonlinear optical susceptibilities of a charged soliton, a neutral soliton, and a polaron in conjugated polymers

Akira Takahashi[a] and Shaul Mukamel
Department of Chemistry, University of Rochester, Rochester, New York 14627

(Received 8 May 1995; accepted 3 July 1995)

The signatures of a charged soliton, a neutral soliton, and a polaron in the resonant and off-resonant optical susceptibilities of conjugated polymers are calculated using the Pariser–Parr–Pople (PPP) model which includes Coulomb interactions. The optical response is obtained by solving equations of motion for the reduced single-electron density matrix, derived using the time dependent Hartree–Fock (TDHF) approximation. The density matrix clearly shows the electronic structures induced by the external field. The roles of charge density, spin density, bond order, and spin bond order waves and how they contribute to the optical response are analyzed. Both charged and neutral solitons show one absorption peak inside the gap of the half-filled case; the frequency of the neutral soliton peak is about 0.7 eV higher than that of a charged soliton. A polaron shows two absorption peaks inside the gap. © *1995 American Institute of Physics.*

I. INTRODUCTION

The photophysics of π-conjugated polymers shows many unique features. These include strong correlation effects because of the low dimensionality, and characteristic elementary excitations such as solitons and polarons.[1–10] These materials exhibit various interesting physical properties including large nonlinear optical susceptibilities, which make them particularly attractive candidates for optical devices.[3,11–15] Numerous theoretical investigations have been carried out on the nonlinear optical response of π-conjugated polymers.[3,6] Most studies are based on the sum over states approach.[16] This method requires the calculation of all the excited states to obtain the nonlinear optical susceptibilities. Since these computations constitute a very difficult many-body problem, exact calculations are limited to small systems with ~12 carbon atoms. However, in order to reproduce the transition from the small molecule limit to the bulk, it is essential to consider systems larger than the coherence length (40 sites in the case of polydiacetylene[17]). The single configuration interaction method which applies when correlation effects are not too strong, can be carried out for larger systems.[18] However, it may not be justified for conjugated polyenes.[8] An additional difficulty with the sum over states method, which further restricts its applicability to small molecules, is the need to perform tedious summations over excited states. Truncating the summations may be dangerous because of the dramatic cancellations resulting from interferences among single exciton and two exciton transitions.[19–21] These interferences make it very difficult to maintain size consistency, i.e., to guarantee that all susceptibilities scale linearly with size for large molecules. Size consistency requires that the approximations involved in ground state and excited state calculations be compatible. This is usually not the case. Consequently, a minor approximation can make a huge effect on the susceptibilities by affecting the delicate balance among large contributions that should cancel. Furthermore, the sum over states method describes optical processes in terms of excitation energies and transition dipole moments. These quantities do not offer an obvious structure–property relation, e.g., what kind of correlation is important, or how characteristic elementary excitations such as solitons affect the optical response.

To overcome these difficulties, we have developed a new method,[22] whereby we calculate the linear and the nonlinear optical response by solving the equations of motion of the reduced single-electron density matrix using the TDHF approximation.[23] The method provides an anharmonic oscillator picture of the optical process and can be easily applied to molecules much larger than the exciton coherence length. Since the TDHF approximation describes small amplitude collective quantum fluctuations around the Hartree–Fock (HF) ground state, as well as the coupling between these fluctuations, it takes into account some important correlation effects beyond the random phase approximation. It is widely accepted that the factorization involved in the TDHF is suitable for describing low energy collective excitations (see, for example, Chapter 12 of Ref. 23). Since linear and nonlinear spectroscopies of conjugated polymers are dominated by such collective excitations, we expect the present approximation to be applicable. For example, the THG spectra of the half-filled polyacetyline can be described well by the present method.[22] Moreover, the interferences and cancellations are naturally built in from the start. This guarantees that size consistency is always maintained even when drastic approximations (e.g., a truncated basis set) are made. The most important advantage of the density matrix approach is that it provides a clear physical picture. In implementing this procedure, we need to calculate the time dependence of the density matrix to obtain linear and nonlinear optical susceptibilities. The density matrix can be expressed using various representations which provide complementary perspectives. These include the real space, the molecular orbital, and the oscillator mode representation.[22] The real space representa-

[a]Present address, Department of Physics, Faculty of Liberal Arts, Yamaguchi University, Japan.

 0021-9606/95/103(16)/7144/12/$6.00

tion allows us to follow directly the charge density, spin density, bond order, and spin bond order fluctuations induced by the external field. Using these quantities, we can explore the electronic structure of the excitations underlying the optical process. The molecular orbital representation describes the nonlinear optical process in terms of motions of electrons and holes with respect to the ground state. Finally, the dynamics of the density matrix can be mapped onto the equations of motion of coupled harmonic oscillators representing electronic normal modes. Using this transformation, we can describe the nonlinear optical process in terms of anharmonic interactions among oscillators.

Most linear and nonlinear spectroscopic studies of conjugated polymers have been limited to molecules with even numbers of carbon atoms and one electron per atom. In this case, half of the molecular orbitals are occupied (this is known as the half-filled band case). In this paper, we extend this method to incorporate charged soliton, neutral soliton or a polaron. Some earlier simple calculations suggest that nonlinear optical susceptibilities are significantly enhanced by introducing a charged soliton.[24] This issue may be relevant to optical devices. Moreover, this problem is of significant fundamental interest as well. It is widely believed that these elementary excitations play important roles in the photophysics of π-conjugated polymers.[1,25] However, despite extensive studies it is not yet possible to identify clearly which excitation is responsible for each specific effect. For example, photoinduced absorption measurements of polyacetylene show that the frequency of the peak of a neutral soliton is about 0.9 eV, higher than that of a charged soliton. The origin of this peak is not fully understood;[26] absorption peaks of a charged and neutral solitons are completely degenerate in frequency for the simple Hückel model without Coulomb interaction. Moreover, the interaction between these elementary excitations and the external electric field is an interesting problem since it can reveal their properties which cannot be observed in the static case.

We adopted the PPP model for π electrons, which includes both short and long range Coulomb interactions. The importance of Coulomb interactions in the nonlinear optics of polyacetylene is widely accepted and many important properties of polyenes can be accounted for by the model.[27–29] Since solitons and polarons have characteristic charge, spin, and bond order distributions, the real space physical picture offered by the present method provides a powerful tool for clarifying the mechanism of the nonlinear response. We found one absorption peak inside the gap of the half-filled case with both charged or neutral solitons, and that the frequency of the neutral soliton peak is about 0.7 eV higher than that of a charged soliton, which is qualitatively consistent with photoinduced absorption measurements. For a polaron, however, there are two absorption peaks inside the gap of the half-filled case. Furthermore, we obtained physical insight on the off-resonant nonlinear optics of these elementary excitations. In a charged soliton we found collective translational oscillation and the coupled fluctuations of the amplitude of the charge density alternation and the soliton width. In a neutral soliton we observed polaronlike charge and spin bond order fluctuations, and coupled fluctuations of the amplitude of the spin density alternation and the soliton width. For a polaron we found collective translational oscillation of a polaron, and the coupled fluctuations of charge density, spin density and spin bond order alternation amplitudes and polaron width.

In Sec. II we introduce the PPP Hamiltonian, and a closed equation of motion for the reduced single particle density matrix is derived in Sec. III using the TDHF approximation. In Sec. IV we present numerical results of first and third order optical susceptibilities and discuss the mechanism of linear and nonlinear optical response using the real space representations of the density matrix.

II. THE PPP HAMILTONIAN

We adopt the PPP Hamiltonian for π electrons. Many properties of polyenes can be reproduced by this Hamiltonian with appropriate parameters.[27] We first introduce the following set of binary electron operators:

$$\hat{\rho}^{\sigma}_{nm}=\hat{c}^{\dagger}_{m,\sigma}\hat{c}_{n,\sigma}, \tag{2.1}$$

where $\hat{c}^{\dagger}_{n,\sigma}(\hat{c}_{n,\sigma})$ creates (annihilates) a π electron of spin σ at the nth carbon atom. These operators satisfy the Fermi anticommutation relation

$$\{\hat{c}^{\dagger}_{m,\sigma},\hat{c}_{n,\sigma'}\}=\delta_{m,n}\delta_{\sigma,\sigma'}. \tag{2.2}$$

Using this notation, the PPP Hamiltonian is given by

$$H=H_{\mathrm{SSH}}+H_C+H_{\mathrm{ext}}. \tag{2.3}$$

H_{SSH} is the Su–Schrieffer–Heeger (SSH) Hamiltonian, which consists of the Hückel Hamiltonian with electron–phonon coupling

$$H_{\mathrm{SSH}}=\sum_{n,m,\sigma} t_{mn}\hat{\rho}^{\sigma}_{nm}+\sum \frac{1}{2}K(x_n-\bar{x})^2. \tag{2.4}$$

Here, t_{mn} is the transfer integral between the nth and mth atoms, K is the harmonic force constant representing the σ bonds, x_n is the deviation of the nth bond length from the mean bond length along the chain axis z, and $\bar{x}$ is the deviation of the equilibrium σ-bond length (in the absence of π electrons) from that mean. We further assume that an electron can hop only between nearest-neighbor atoms. Thus

$$t_{nn+1}=t_{n+1n}=\bar{\beta}-\beta' x_n, \tag{2.5}$$

and $t_{mn}=0$ otherwise. $\bar{\beta}$ is the mean transfer integral and β' is the electron–phonon coupling constant.

H_C represents the electron–electron Coulomb interactions and is given by

$$H_C=\sum_n U\hat{\rho}^{\uparrow}_{nn}\hat{\rho}^{\downarrow}_{nn}+\frac{1}{2}\sum_{n,m,\sigma,\sigma'}^{n\neq m}\gamma_{nm}\hat{\rho}^{\sigma}_{nn}\hat{\rho}^{\sigma'}_{mm}. \tag{2.6}$$

An on-site (Hubbard) repulsion U is given by

$$U=\frac{U_0}{\epsilon}, \tag{2.7}$$

and a repulsion between the nth and the mth sites γ_{nm} is given by the Ohno formula

$$\gamma_{nm}=\frac{U}{\sqrt{1+(r_{nm}/a_0)^2}}, \tag{2.8}$$

where $U_0=11.13$ eV is the unscreened on-site repulsion, ϵ is the dielectric constant which describes the screening by σ electrons, r_{nm} is the distance between nth and mth sites, and $a_0=1.2935$ Å. These parameters reproduce the correct energy gap for polyacetylene (2.0 eV): $\beta=-2.4$ eV, $\beta'=-3.5$ eV Å^{-1}, $K=30$ eV Å^{-2}, $\bar{x}=0.14$ Å, and $\epsilon=1.5$.

$H_{\rm ext}$ represents the coupling between the π electrons and the external electric field $E(t)$ polarized along the chain axis z. Within the dipole approximation we then have

$$H_{\rm ext}=-E(t)\hat{P}, \tag{2.9}$$

where $\hat{P}$ is the molecular polarization operator

$$\hat{P}=-e\sum_{n,\sigma} z(n)\hat{\rho}^{\sigma}_{nn}, \tag{2.10}$$

$-e$ is the electron charge and $z(n)$ is the z coordinate of nth atom.

III. EQUATIONS OF MOTION FOR THE REDUCED DENSITY MATRIX

In this section, we briefly review the procedure developed in Ref. 22 for calculating the nonlinear optical susceptibilities. Starting with the Schrödinger equation, the equation of motion of the expectation value of our binary electron operators

$$i\rho^{\sigma}(t)=\langle\Psi(t)|\hat{\rho}^{\sigma}|\Psi(t)\rangle, \tag{3.1}$$

is given by

$$\hbar\dot{\rho}^{\sigma}(t)=\langle\Psi(t)|[\hat{\rho}^{\sigma},H]|\Psi(t)\rangle, \tag{3.2}$$

where $|\Psi(t)\rangle$ is the total many-electron wave function of the system. The expectation values ρ^{σ}_{nm} can be interpreted as elements of the reduced single-electron density matrix.[30–32]

Utilizing the commutation relations (2.2), we can calculate the rhs of Eq. (3.2). These equations of motion are exact but not closed. By assuming that $|\Psi(t)\rangle$ can be represented by a single Slater determinant at all times (the TDHF approximation),[23] then the two-electron densities can be factorized into products of single electron densities and the equations are closed. This results in the TDHF equation

$$i\hbar\dot{\rho}^{\sigma}(t)=[h^{\sigma}(t)+f(t),\rho^{\sigma}(t)], \tag{3.3}$$

where h^{σ} is the Fock operator matrix corresponding to $H_{\rm SSH}+H_C$ with spin σ

$$h^{\sigma}_{nm}(t)=t_{nm}+\delta_{n,m}\sum_{l,\sigma'}\gamma_{nl}\rho^{\sigma'}_{ll}(t)-\gamma_{nm}\rho^{\sigma}_{nm}(t), \tag{3.4}$$

and $f_{nm}(t)$ is the Fock operator matrix corresponding to $H_{\rm ext}$

$$f_{nm}(t)=\delta_{n,m}ez(n)E(t). \tag{3.5}$$

We have solved these equations of motion by expanding the single electron density matrix in powers of the external field.[33] The zeroth order solution was taken to be the stationary HF density matrix, which satisfies

$$[h^{\sigma},\rho^{\sigma}]=0. \tag{3.6}$$

The HF equation was solved numerically by an iterative diagonalization. The geometry x_n can be determined by employing the force equilibrium condition as shown in Ref. 22

$$\frac{\partial\langle|\psi_{\rm HF}|H|\psi_{\rm HF}\rangle}{\partial x_n}=0, \tag{3.7}$$

where $|\psi_{\rm HF}\rangle$ is the HF wave function and $n=1,...,N-1$. Using the Hellman–Feynmann theorem, the force equilibrium condition assumes the form

$$K(x_n-\bar{x})-4\beta'\bar{\rho}_{n,n+1}=0. \tag{3.8}$$

In this paper, we work with a fixed geometry and do not incorporate nuclear motions. This is justified for the off-resonant response. However, it is straightforward to take lattice dynamics into account in our formalism.

To compute the nonlinear optical polarizabilities, we expand ρ in powers of the external field, where the density matrix ρ is defined by

$$\rho=\begin{bmatrix}\rho^{\uparrow} & 0\\ 0 & \rho^{\downarrow}\end{bmatrix}. \tag{3.9}$$

The expansion is given by

$$\rho(t)=\bar{\rho}+\rho^{(1)}(t)+\rho^{(2)}(t)+\rho^{(3)}(t)+\cdots, \tag{3.10}$$

where $\bar{\rho}$ is the density matrix of the HF solution and $\rho^{(q)}(t)$ is the qth order density matrix of the TDHF solution. The Fock operator matrix is further expanded in powers of the external field

$$h(t)=\bar{h}+h^{(1)}(t)+h^{(2)}(t)+h^{(3)}(t)+\cdots, \tag{3.11}$$

where $\bar{h}$ is Fock-operator matrix of the HF solution, h is defined from h^{σ} as Eq. (3.9) and

$$h^{\sigma(q)}_{nm}(t)=\delta_{n,m}\sum_{l,\sigma'}\gamma_{nl}\rho^{\sigma'(q)}_{ll}(t)-\gamma_{nm}\rho^{\sigma(q)}_{nm}(t). \tag{3.12}$$

Substituting Eqs. (3.10) and (3.11) into Eqs. (3.3), we obtain the first, the second, and the third order equations of motions. Taking the Fourier transform of these equations defined by

$$g(\omega)\equiv\frac{1}{\sqrt{2\pi}}\int_{-\infty}^{+\infty}g(t)\exp(i\omega t)dt, \tag{3.13}$$

where $g(t)$ is an arbitrary function of t, we recast the equations of motions in the frequency domain

$$\rho^{(1)}(\omega)=G(\omega)[f(\omega),\bar{\rho}], \tag{3.14a}$$

$$\rho^{(2)}(\omega)=G(\omega)\frac{1}{\sqrt{2\pi}}\int_{-\infty}^{+\infty}\{[h^{(1)}(\omega'),\rho^{(1)}(\omega-\omega')]+[f(\omega'),\rho^{(1)}(\omega-\omega')]\}d\omega', \tag{3.14b}$$

$$\rho^{(3)}(\omega)=G(\omega)\frac{1}{\sqrt{2\pi}}\int_{-\infty}^{+\infty}\{[h^{(1)}(\omega'),\rho^{(2)}(\omega-\omega')]+[h^{(2)}(\omega'),\rho^{(1)}(\omega-\omega')]+[f(\omega'),\rho^{(2)}(\omega-\omega')]\}d\omega'. \tag{3.14c}$$

The Liouville space (tetradic) Green function $G(\omega)$ is defined by

$$G^{-1}_{ij,mn}(\omega)=\hbar\omega\delta_{i,m}\delta_{j,n}-L_{ij,mn}(\omega). \tag{3.15}$$

where L is defined from L^{σ} as in Eq. (3.9) and

$$L^{\sigma}_{ij,mn}(\omega)=\delta_{j,n}\bar{h}_{im}-\delta_{i,m}\bar{h}_{jn}+\delta_{m,n}(\gamma_{in}-\gamma_{jn})(\bar{\rho}^{\uparrow}_{ij}+\bar{\rho}^{\downarrow}_{ij}) - \delta_{i,m}\gamma_{in}\bar{\rho}^{\sigma}_{jn}+\delta_{j,n}\gamma_{jm}\bar{\rho}^{\sigma}_{im}. \tag{3.16}$$

This way, we can obtain the TDHF solution iteratively to arbitrary order in the external field.

The expectation value of the total polarization operator of a single molecule $P(t)=\langle\Psi(t)|\hat{P}|\Psi(t)\rangle$ is given by

$$P(t)=-e\sum_{n,\sigma} z(n)\rho^{\sigma}_{nn}(t). \tag{3.17}$$

We shall expand $P(t)$ in powers of the external field

$$P(t)=P^{(1)}(t)+P^{(2)}(t)+P^{(3)}(t)+\cdots, \tag{3.18}$$

where $P^{(q)}(t)$ is the total polarization to qth order and $P^{(0)}(t)=0$. From Eqs. (3.10) and (3.17), it follows that

$$P^{(q)}(t)=-e\sum_{n,\sigma} z(n)\rho^{\sigma(q)}_{nn}(t), \tag{3.19}$$

where $\rho^{(q)}_{n,n}(t)$ is obtained by taking the inverse Fourier transform of $\rho^{(q)}_{nn}(\omega)$.

Following the procedure described earlier, we obtain the single electron density matrices induce by the external field $E(t)=E_1\cos\omega_1 t$ order by order in the field (for details, see Ref. 22)

$$\rho^{(1)}(t)=\frac{1}{\sqrt{2\pi}}\{\mathrm{Re}[\tilde{\rho}^{(1)}(-\omega_1;\omega_1)]\cos(\omega_1 t) + \mathrm{Im}[\tilde{\rho}^{(1)}(-\omega_1;\omega_1)]\sin(\omega_1 t)\}, \tag{3.20a}$$

$$\rho^{(2)}(t)=\frac{1}{\sqrt{2\pi}}\{\mathrm{Re}[\tilde{\rho}^{(2)}(-2\omega_1;\omega_1,\omega_1)]\cos(2\omega_1 t) + \mathrm{Im}[\tilde{\rho}^{(2)}(-2\omega_1;\omega_1,\omega_1)]\sin(2\omega_1 t)+\cdots\}, \tag{3.20b}$$

$$\rho^{(3)}(t)=\frac{1}{\sqrt{2\pi}}\{\mathrm{Re}[\tilde{\rho}^{(3)}(-3\omega_1;\omega_1,\omega_1,\omega_1)]\cos(3\omega_1 t) + \mathrm{Im}[\tilde{\rho}^{(3)}(-3\omega_1;\omega_1,\omega_1,\omega_1)]\sin(3\omega_1 t)+\cdots\}. \tag{3.20c}$$

We have kept only terms which contribute to $\gamma(-3\omega_1;\ \omega_1,\ \omega_1,\ \omega_1)$, and all other terms were omitted in these expressions since we focus on third harmonic generation (THG).

The single electron density matrices have a term oscillating in phase with the external electric field and a term oscillating out of the phase. The amplitudes of the former terms are given by $\mathrm{Re}[\tilde{\rho}^{(q)}]$ and they contribute to the real parts of the linear and nonlinear polarizabilities, and those of the latter terms are given by $\mathrm{Im}[\tilde{\rho}^{(q)}]$ and they contribute to the imaginary parts.

Using $P^{(q)}(t)$ and $\rho^{(q)}(\omega)$, we obtain our final expressions for the optical polarizabilities

$$\alpha(-\omega;\omega)=\frac{1}{E_1}\frac{2e}{\sqrt{2\pi}}\sum_{n,\sigma} z(n)\tilde{\rho}^{\sigma(1)}_{n,n}(-\omega;\omega), \tag{3.21}$$

$$\gamma(-3\omega;\omega,\omega,\omega)=-\frac{1}{E_1^3}\frac{2e}{\sqrt{2\pi}}\sum_{n,\sigma} z(n)\tilde{\rho}^{\sigma(3)}_{n,n}(-3\omega;\omega,\omega,\omega). \tag{3.22}$$

Equation (3.22) gives the third order polarizability responsible for THG. Other four wave mixing processes can be described by simply changing the frequency arguments. The present calculation can be also directly extended to higher nonlinearities.

IV. OPTICAL RESPONSE AND ELEMENTARY DENSITY WAVES

In this section, we apply the anharmonic oscillator density-matrix approach to four cases: we first study the half-filled case, which is used as a reference, and then consider chains with a charged soliton, a neutral soliton, or a polaron. We shall consider the following four important physical quantities which characterize the electronic structure of the system. These are the charge density (d_n) and spin density (s_n) at the nth atom, and bond order (p_n) and spin bond order (t_n) at the nth bond,

$$\begin{aligned} d_n&=1-\sum_{\sigma}\rho^{\sigma}_{n,n},\\ s_n&=\tfrac{1}{2}(\rho^{\uparrow}_{n,n}-\rho^{\downarrow}_{n,n}),\\ p_n&=\frac{1}{2}\sum_{\sigma}(\rho^{\sigma}_{n,n+1}+\rho^{\sigma}_{n+1,n}),\\ t_n&=\tfrac{1}{4}(\rho^{\uparrow}_{n,n+1}+\rho^{\uparrow}_{n+1,n}-\rho^{\downarrow}_{n,n+1}-\rho^{\downarrow}_{n+1,n}). \end{aligned} \tag{4.1}$$

Fukutome and co-workers[4,5] have carried out a mean field study of the half-filled PPP model and found four regular density wave states that can represent the HF ground state for a suitable choice of parameters. These states are related to the four important physical quantities introduced above. They are charge density wave (CDW), spin density wave (SDW), bond order wave (BOW), and spin bond order wave (SBOW), where the corresponding quantities alternate between every adjacent two sites or bonds. We further introduce the bond order parameter, which measures the alternating component of bond order, namely, the strength of bond order alternation

$$p'_n\equiv(-1)^{n-1}(p_n-\bar{p}), \tag{4.2}$$

where p is the average bond order obtained from Eq. (3.8) as

$$\bar{p}=-\frac{K\bar{x}}{2\beta'}. \tag{4.3}$$

It follows from Eq. (3.8), that the bond order parameter is proportional to the bond length alternation strength (lattice order parameter). Thus the bond order parameter is most suitable for identifying soliton or polaron like electronic structures, as will be shown below. Note also that the total polarization is determined by the charge density, as can be seen from Eq. (3.17). We have added a damping term

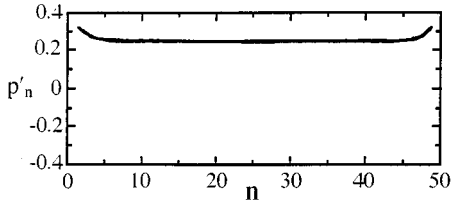

FIG. 1. The bond order parameter distribution of the Hartree–Fock ground state of the half-filled chain.

(0.1 eV) to the TDHF equation as described in Ref. 22. This provides a finite linewidth to the optical resonances and can represent a simple line broadening mechanism (e.g., due to coupling with phonons) or a finite spectral resolution.

We first discuss the half-filled linear chain with 50 sites and 25 up and 25 down spin electrons. The geometry-optimized HF ground state of the present Hamiltonian is BOW, where p_n alternates between each adjacent two bonds, and the other important physical quantities vanish. The HF ground state has an almost uniform bond order parameter ($p_n'=0.24$), as shown in Fig. 1. Because of boundary effects, the bond order parameter increases slightly near the chain edge. As indicated earlier, this parameter is proportional to the bond length alternation strength, which gives the alternation of the transfer integral as seen from Eq. (2.5). Thus, the transfer integral β_n can be approximated by $\beta_n=\beta\{1-(-1)^n\delta\}$ where $\delta=0.082$, except for the edge region. The BOW structure is stabilized by the exchange Coulomb, and the electron–phonon interactions.[27]

In Fig. 2, we display the linear absorption ($\mathrm{Im}[a(-\omega;\omega)]$) and the absolute magnitude of the third order polarizability responsible for THG ($|\gamma(-3\omega;\omega,\omega,\omega)|$). We label the resonances in the absorption spectra by A–C. We next examine the electronic structure induced by the external electric field $E=E_1\cos\omega_1 t$. The charge density which is related to the diagonal elements of the density matrix in the

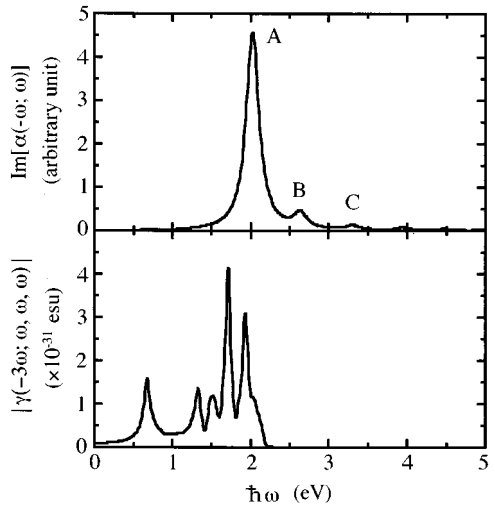

FIG. 2. The linear absorption spectrum $\mathrm{Im}[\alpha(-\omega;\omega)]$ and the THG hyperpolarizability $|\gamma(-3\omega;\omega,\omega,\omega)|$ of the half-filled chain are plotted versus frequency ω.

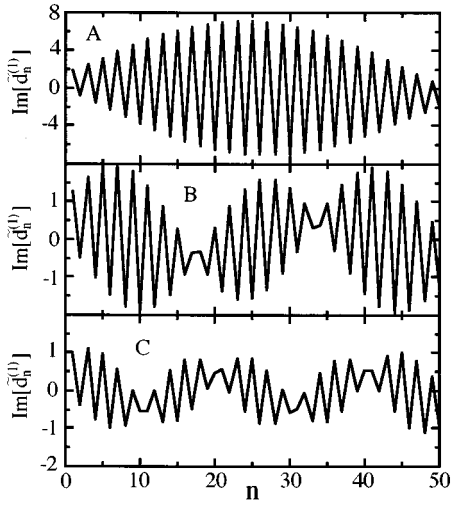

FIG. 3. The first order amplitude of the charge density oscillation induced by the external field at the frequencies of the absorption peaks A, B, and C in the half-filled chain. We show only the amplitudes $\mathrm{Im}[\tilde{d}_n^{(1)}]$ oscillating out of phase with the external field. The applied external electric field is 10^8 V/m.

real space representation has terms oscillating in phase and out of the phase with respect to the external electric field,

$$d_n^{(q)}(t)=\frac{1}{\sqrt{2\pi}}\{\mathrm{Re}[\tilde{d}_n^{(q)}(q\omega_1)]\cos(q\omega,t) + \mathrm{Im}[\tilde{d}_n^{(q)}(q\omega_1)]\sin(q\omega_1 t)+\cdots\}, \tag{4.4}$$

and

$$\tilde{d}_n^{(q)}(q\omega_1)=-\tilde{\rho}_{nn}^{\uparrow(q)}(-q\omega_1;\cdots)-\tilde{\rho}_{nn}^{\downarrow(q)}(-q\omega_1;\cdots). \tag{4.5}$$

The spin density, bond order and spin bond order parameter induced by the external field also have in-phase and out-of-phase components, and their amplitudes are given by

$$\tilde{s}_n^{(q)}(q\omega_1)=\tfrac{1}{2}\{\tilde{\rho}_{nn}^{\uparrow(q)}(-q\omega_1;\cdots)-\tilde{\rho}_{nn}^{\downarrow(q)}(-q\omega_1;\cdots)\}, \tag{4.6}$$

$$\tilde{p}_n^{(q)}(q\omega_1)=\tfrac{1}{2}(-1)^{n-1}\{\tilde{p}_{nn+1}^{\uparrow(q)}(-q\omega_1;\cdots) + \tilde{p}_{n+1n}^{\uparrow(q)}(-q\omega_1;\cdots)+\tilde{p}_{nn+1}^{\downarrow(q)}(-q\omega_1;\cdots) + \tilde{p}_{n+1n}^{\downarrow(q)}(-q\omega_1;\cdots)\}, \tag{4.7}$$

$$\tilde{t}_n^{(q)}(q\omega_1)=\tfrac{1}{4}\{\tilde{\rho}_{nn+1}^{\uparrow(q)}(-q\omega_1;\cdots)+\tilde{\rho}_{n+1n}^{\uparrow(q)}(-q\omega_1;\cdots) - \tilde{\rho}_{nn+1}^{\downarrow(q)}(-q\omega_1;\cdots) - \tilde{\rho}_{n+1n}^{\downarrow(q)}(-q\omega_1;\cdots)\}. \tag{4.8}$$

To analyze the electronic dynamics underlying the absorption spectrum, we investigated the first order electronic structure induced by the external field. In Fig. 3 we show $\mathrm{Im}[\tilde{d}_n^{(1)}]$ at the three dominant absorption peak frequencies (A, B, and C). Only the imaginary parts which are strongly enhanced at resonance frequencies are shown. However, the charge–density distributions of the real and the imaginary parts are very similar at all frequencies. The other three important physical quantities, (s, p, and t) vanish in first order

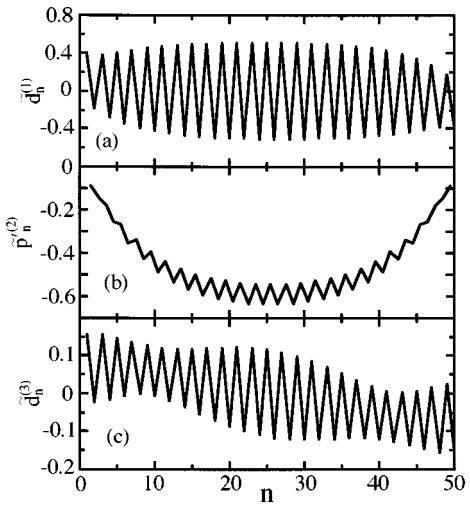

FIG. 4. (a) The first order amplitude of charge density oscillation, (b) the second order amplitude of bond order parameter oscillation, and (c) the third order amplitude of charge density oscillation induced by the external field with $\omega=0$ in the half-filled chain. The applied external electric field is 10^8 V/m.

because of symmetry. At the frequencies of the A, B, and C peaks, the induced charge distributions have CDW like structures with zero, two and four nodes, respectively; the number of nodes increases by two from one peak to the next as the frequency is increased. Thus the absorption spectrum is dominated by the series of the characteristic CDW-like charge density fluctuations. These absorption peaks lie below the HF energy gap, and these charge density fluctuations can, therefore, be regarded as excitons. However, these excitons are not simple electron–hole pairs but reflect the characteristic collective nature of the electronic structure of one-dimensional systems. The frequency dispersed absorption and THG spectra calculated in Ref. 22 for a chain with 60 atoms are very similar to the ones reported here for a 50 atom chain. This reflects the size consistency of the present approach.

We next consider the off-resonant $|\gamma(-3\omega;\omega,\omega,\omega)|$ with $\omega=0$. We shall denote it as $|\gamma(0)|$. In Fig. 4 we display the induced electronic structure to first, second and third order in the external field. We only show $\tilde{d}_n^{(q)}(q\omega_1)$ in the first and third orders, and $\tilde{p}_n'^{(q)}$ in the second order because the other important physical quantities vanish. Note that these quantities are real for $\omega=0$. These properties follow directly from the symmetry of our Hamiltonian. In first order, we see CDW-like fluctuations with zero node. This type of charge density fluctuation is dominant because it has the largest oscillator strength. In second order, we can observe the characteristic soliton pair like bond order oscillation pattern. This type of bond order oscillation dominates the second order response since its coupling with CDW-like fluctuation with zero node, which is dominant in first order, is the strongest. This can be seen more clearly when we use the harmonic oscillator representation.[22] We also see collective CDW-like fluctuations with zero node in the third order response.

We now turn to the charged soliton case, and consider a chain with 49 sites and 24 up and down spin electrons. The

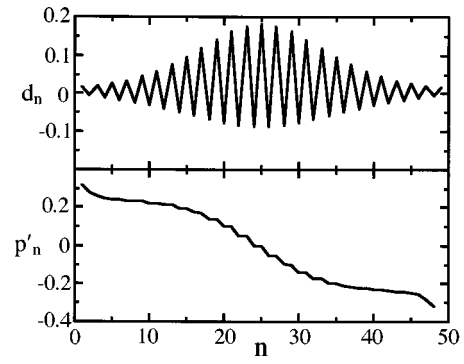

FIG. 5. The charge density and bond order parameter distributions of the Hartree–Fock charged soliton solution.

HF ground state electronic structure is shown in Fig. 5. The following electronic structures characteristic of a charged soliton are observed:[4] (1) CDW-like structures around the soliton center; and (2) the phase of bond order alternation is reversed at the soliton center. In Fig. 6, we display the linear absorption and the absolute value of the third order THG polarizability. In the half-filled chain (Fig. 2), neighboring peaks form an almost harmonic ladder with a very similar frequency interval. In contrast, for a charged soliton, peak A has a much lower frequency than the other peaks; and its frequency is about half the frequency of the lowest peak of the half-filled chain. This one of the most striking features of solitons is clearly reproduced by the present theory. To analyze the charge dynamics underlying the absorption spectra, we investigated the first order electronic structure induced by the external field. In Fig. 7 we display $\mathrm{Im}[\tilde{d}_n^{(1)}]$ and $\mathrm{Im}[\tilde{p}'^{(1)}_n]$ at the frequency of the strongest absorption peak A. Note that the other three important physical quantities vanish in first order because of symmetry. At this frequency, the induced charge distributions have again CDW-like structures. However, unlike the lowest peak of the half-filled chain, they have one node. The induced bond order parameter oscillation has zero nodes. The number of these nodes increases by two from one peak to the next as the frequency is increased. At

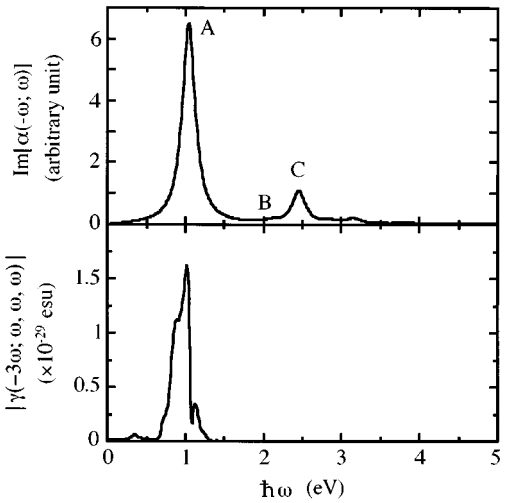

FIG. 6. The same physical quantities as Fig. 2, but for a charged soliton.

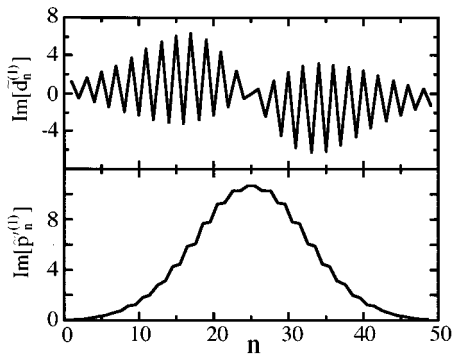

FIG. 7. The first order amplitude of the charge density and bond order parameter oscillations induced by the external field at the frequency of the absorption peak A of a charged soliton. We show only the amplitudes oscillating out of phase with respect to the external field. The applied external electric field is 10^8 V/m.

the frequencies of peaks B and C, the induced CDW-like charge distributions have three and five nodes, respectively, and the induced bond order parameter oscillation has two and four nodes, respectively. This is similar to the half-filled chain. However, peak A has an interesting physical property in this case; by comparing the electronic structure of the HF ground state and first order density matrix induced at the frequency of peak A, we see that the alternating component of the first order charge density and first order bond order parameter induced by the external field closely resemble the derivative of the corresponding HF solution. This indicates that the lowest peak A results from the collective oscillation of the position of a charged soliton. Therefore, the peak has a much lower frequency and larger oscillator strength compared with the other peaks. Note that since the lattice is frozen, the frequency of the collective motion is not zero.

We next turn to the third order susceptibility $|\gamma(0)|$. In Fig. 8 we show the induced density matrices to first, second and third order in the external field. Only $\tilde{d}_n^{(q)}$ and $\tilde{p}'^{(q)}_n$ are displayed because the other four important physical quantities vanish. In first order, we observe the collective translational oscillation of a charged soliton. This type of charge density and bond order fluctuations are dominant because they have the largest oscillator strength. In second order, the distribution of $\tilde{d}_n^{(2)}$ is similar to the charge density distribution of the charged soliton HF solution (Fig. 5). We can thus view the induced fluctuation as the oscillation of the charge density alternation amplitude of a charged soliton. Moreover, by comparing the $\tilde{p}_n'^{(2)}$ distribution with the p_n' distribution of the HF charged soliton solution, we see that oscillations of the soliton width are induced as well in second order. This type of fluctuation is dominant because its coupling with the translational oscillation of a charged soliton, which is the dominant fluctuation induced in the first order, is the strongest. We again see the collective oscillation of the position of a charged soliton in third order.

We next examine the neutral soliton by studying a chain with 49 sites and 25 up and 24 down spin electrons. The electronic structure of the HF ground state of this system is shown in Fig. 9. The following electronic structures characteristic of a neutral soliton are observed:[4] (1) SDW-like pat-

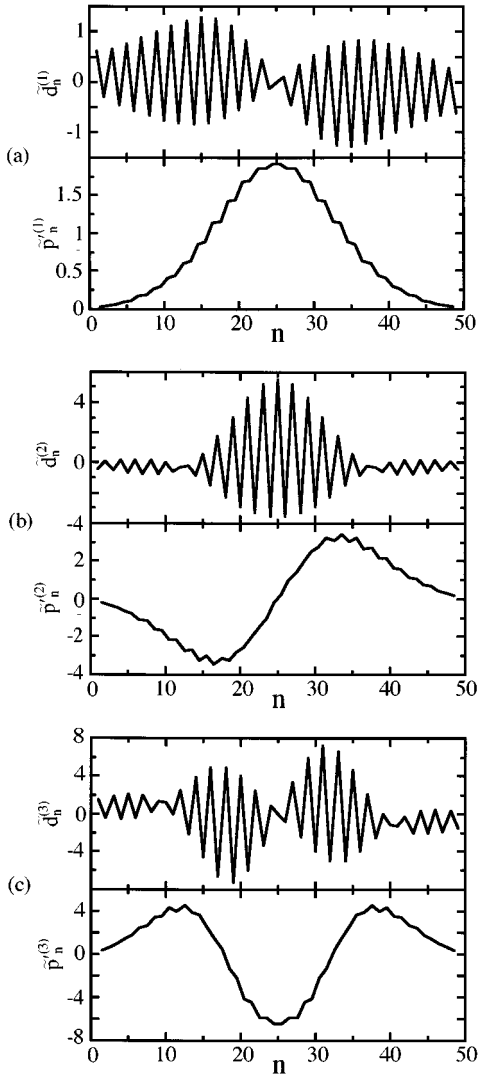

FIG. 8. (a) The first order, (b) the second order, and (c) the third order amplitudes of charge density and bond order parameter oscillations induced by the external field with $\omega=0$ in a charged soliton. The applied external electric field is 10^8 V/m.

tern around the soliton center; (2) the phase of bond order alternation is reversed at the soliton center. In Fig. 10, we display the linear absorption and the absolute value of the THG third order polarizability. The second lowest peak B

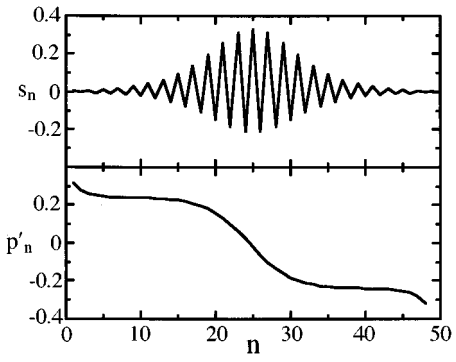

FIG. 9. The spin density and bond order parameter distributions of the Hartree–Fock neutral soliton solution.

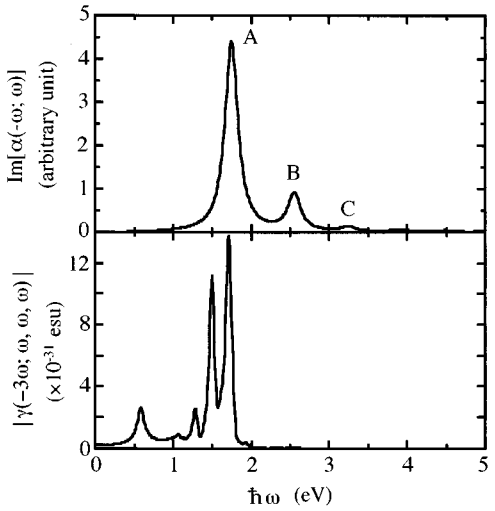

FIG. 10. The same physical quantities as Fig. 2, but for a neutral soliton.

appears at about the same frequency as that of the corresponding peak of the half-filled chain, but the lowest peak A is inside the gap of the half-filled chain, similar to the charged soliton. This one of the most important features of solitons is clearly described by the present theory. The frequency of the lowest peak of a neutral soliton is about 0.7 eV higher than that of the corresponding peak of a charged soliton. This is in contrast to the Hückel model where they have the same frequency. Our result is qualitatively consistent with the photoinduced absorption experiment.[26] To analyze the charge dynamics underlying the absorption spectra, we investigated the first order electronic structure induced by the external field. In Fig. 11 we show $\mathrm{Im}[\tilde{d}_n^{(1)}]$ and $\mathrm{Im}[\tilde{t}_n^{(1)}]$ at the frequencies of the strongest absorption peak A. All other important physical quantities vanish in first order because of symmetry. At the lowest peak A frequency, the induced charge distributions have a CDW-like structure with one node, and the induced spin bond order distributions have SBOW-like structure with zero node; the induced electronic structure is similar to the charge and spin bond order distribution of the HF polaron solution (see Fig. 13). Therefore,

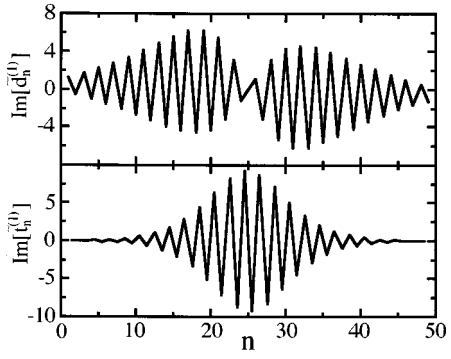

FIG. 11. The first order amplitude of the charge density and spin bond order oscillations induced by the external field at the frequency of the absorption peak A of a neutral soliton. Only the amplitudes oscillating out of phase with respect to the external field are shown. The applied external electric field is 10^8 V/m.

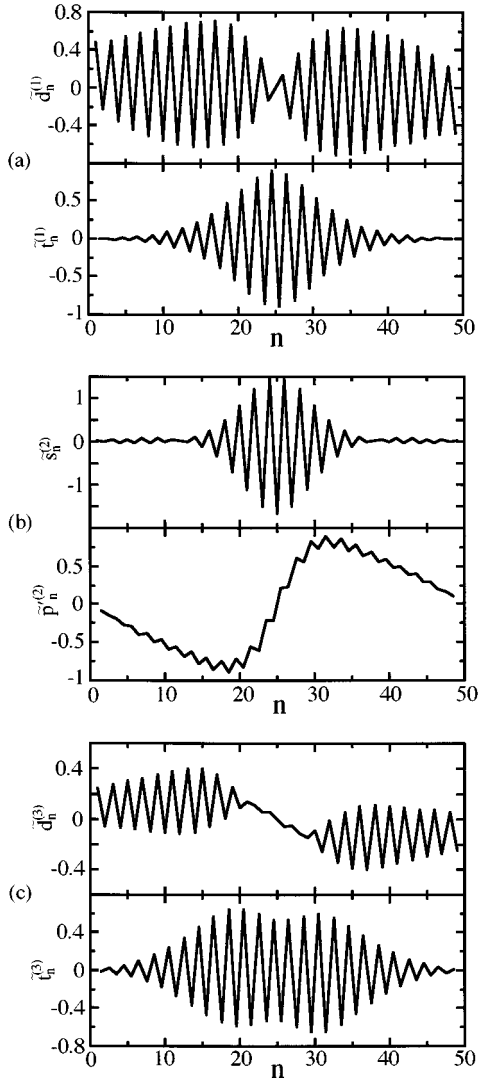

FIG. 12. (a) The first order amplitude of charge density and spin bond order oscillations, (b) the second order amplitude of spin density and bond order parameter oscillations, and (c) the third order amplitude of charge density and spin bond order oscillations induced by the external field with $\omega=0$ in a neutral soliton. The applied external electric field is 10^8 V/m.

the nature of the absorption process of a neutral soliton and that of a charged soliton is completely different, and the degeneracy of the absorption peak between charged and neutral solitons exists only in the Hückel model. We now consider the off-resonant $|\gamma(0)|$. In Fig. 12 we show the induced electronic structure in first, second, and third order in the external field. We show only $\tilde{d}_n^{(q)}$ and $\tilde{t}_n^{(q)}$ in the first and third orders and $\tilde{s}_n^{(q)}$ and $\tilde{p}_n'^{(q)}$ in the second order because the other important physical quantities vanish. In first order, we see polaronlike charge and spin bond order distributions. This type of charge density and spin bond order fluctuations are dominant because they have the largest oscillator strength. In second order, using similar arguments as for the charged soliton case, we can regard the induced electronic structure as the amplitude oscillation of spin density alternation of a neutral soliton, and the oscillation of the soliton width. This fluctuation is dominant since its coupling with polaronlike charge density and spin bond order fluctuation,

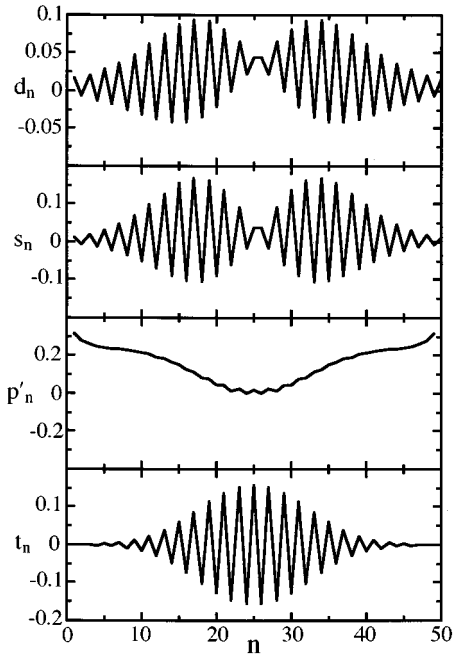

FIG. 13. The charge density, spin density, bond order parameter, and spin bond order distributions of the Hartree–Fock polaron solution.

which is the most significant in the first order, is the strongest. We again see polaron like charge density and spin bond order fluctuation in third order.

To study the polaron case, we considered a chain with 50 sites and 25 up and 24 down spin electrons. The electronic structure of the HF ground state is shown in Fig. 13. The following electronic structures characteristic of a polaron are observed:[5] (1) CDW and SDW-like electronic structure with one node around the polaron center; (2) SBOW-like electronic structure with zero node around the polaron center; (3) the bond order alternation amplitude becomes weak but the phase of bond order alternation is not reversed at the polaron center. In Fig. 14, we display the linear absorption and the absolute magnitude of the third order polarizability connected to THG. There exist two large peaks inside the gap of the half-filled chain but they are not well resolved with the present damping rate. In the Hückel model, the calculated absorption of a polaron shows three absorption peaks inside the gap, where one of them is very weak. This very weak peak is absent in the present calculation. This is consistent with the single CI calculation of the PPP model.[34] To analyze the charge dynamics underlying the absorption spectra, we investigated the first order electronic structure induced by the external field. In Fig. 15, we show Im$[\tilde{d}_n^{(1)}]$, Im$[\tilde{s}_n^{(1)}]$, Im$[\tilde{p}_n'^{(1)}]$, and Im$[\tilde{t}_n^{(1)}]$ at the frequencies of peaks A and B. At the frequency of the lowest peak A (the second lowest peak B), we observe the following electronic structure induced by the external field: (1) CDW-like charge distributions with two nodes (zero node); (2) SDW-like spin distributions with two nodes (zero node). This is in contrast to the previous cases of a half-filled chain, a charged soliton and a neutral soliton, where the second lowest peak has two more nodes in these physical quantities compared with the lowest peak. We can rationalize this difference as follows. By comparing the electronic structure of the HF polaron solution and the first order electronic structure induced at the frequency of peak A, we see that the alternating components of Im$[\tilde{d}_n^{(1)}]$, Im$[\tilde{s}_n^{(1)}]$, Im$[\tilde{t}_n^{(1)}]$, and Im$[\tilde{p}_n'^{(1)}]$ have derivativelike shape of the corresponding polaron solution. This indicates that the lowest peak A results from a collective translational oscillation of a polaron. Therefore, peak A has a lower frequency, a larger oscillator strength and more nodes than peak B. Note that since the lattice is frozen, the collective motion frequency is not zero.

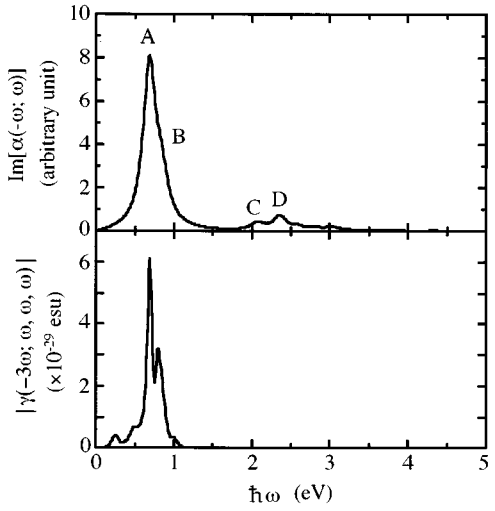

FIG. 14. The same physical quantities as Fig. 2, but for a polaron.

We next consider the off-resonant $|\gamma(0)|$. In Figs. 16, 17, and 18 we show the induced four important physical quantities to first, second, and third order in the external field. In first order, we observe an electronic structure similar to that induced at the frequency of peak A; charge (spin) distribution has CDW (SDW)-like structure with three loops. However, unlike the first order electronic structure induced at the peak A frequency, the charge density (spin density) alternation amplitude of the central loop (two loops at both ends) is much smaller than the other ones. The reason is that although the electronic fluctuation responsible for peak A has the largest contribution in first order, that responsible to the peak B also has large contributions as shown in the following. In the central part of the chain, alternating charge density (spin density) pattern of these fluctuations responsible for peaks A and B interfere destructively (constructively) so that the amplitude of alternating charge density (spin density) pattern becomes small (large). At both ends of the chain, the amplitude of alternating charge density (spin density) pattern becomes large (small) due to constructive (destructive) interference. In the second order, by comparing with the HF polaron solution (see Fig. 13), we see that the distributions of $\tilde{d}_n^{(2)}$, $\tilde{s}_n^{(2)}$, and $\tilde{t}_n^{(2)}$ are similar to those of d_n, s_n, and t_n of the HF polaron solution, respectively. Thus the induced fluctuations can be interpreted as the oscillations of charge density, spin density, and spin bond order alternation amplitudes of a polaron, as shown in the case of a charged soliton. From the distribution of $\tilde{p}_n'^{(2)}$, we see that the primary induced oscillation is of a polaron width. This type of fluctuation is dominant in second

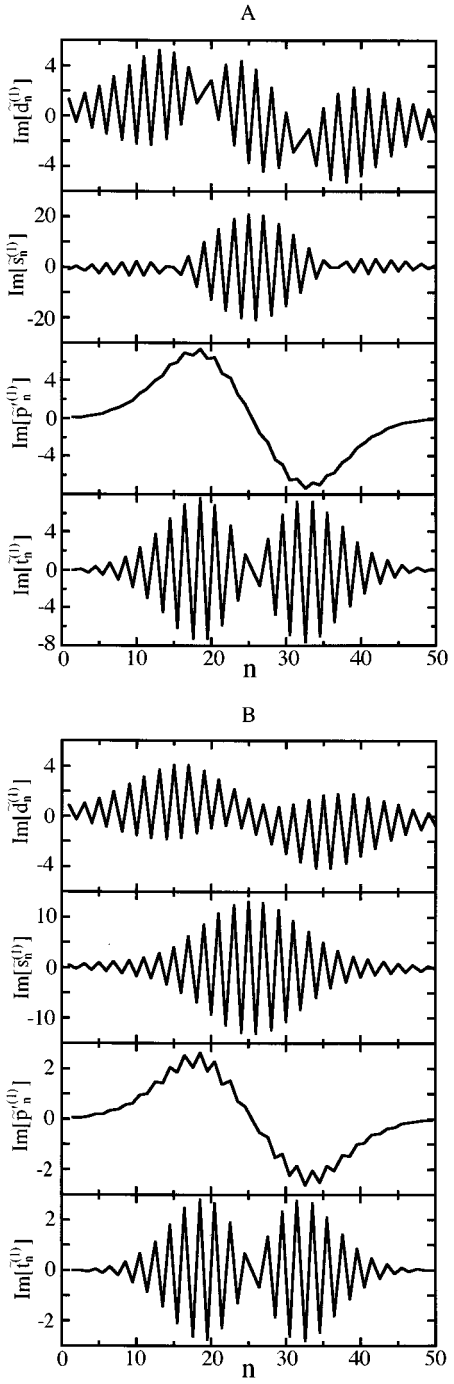

FIG. 15. The first order amplitude of the charge density, spin density, bond order parameter, and spin bond order oscillations induced by the external field at the frequencies of the absorption peaks A and B of a polaron. We show only the amplitudes oscillating out of phase with respect to the external field. The applied external electric field is 10^8 V/m.

order because its coupling with translational oscillation of a polaron, which is dominant in first order, is the strongest. In third order, we see an induced electronic structure similar to that of the first order. Thus, the collective translational oscillation of a polaron is the largest fluctuation also in third order, but the electronic fluctuations responsible for peak B also have large contributions, as shown earlier.

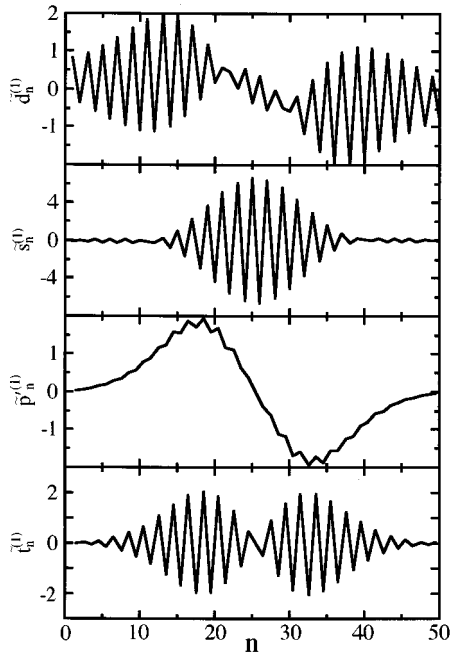

FIG. 16. The first order amplitude of charge density, spin density, bond order parameter and spin bond order oscillations induced by the external field with $\omega=0$ in a polaron. The applied external electric field is 10^8 V/m.

V. DISCUSSION

We have studied the linear and nonlinear susceptibilities of the half-filled regular chain using the anharmonic oscillator approach.[22] The values of the static third order polarizability $\gamma(0)$ for the regular chain, charged soliton, neutral soliton, and polaron are 9.09×10^{-33}, 7.83×10^{-32}, 1.95×10^{-32}, and 8.90×10^{-32} esu, respectively. The essential differences between the regular chain and a charged soliton,

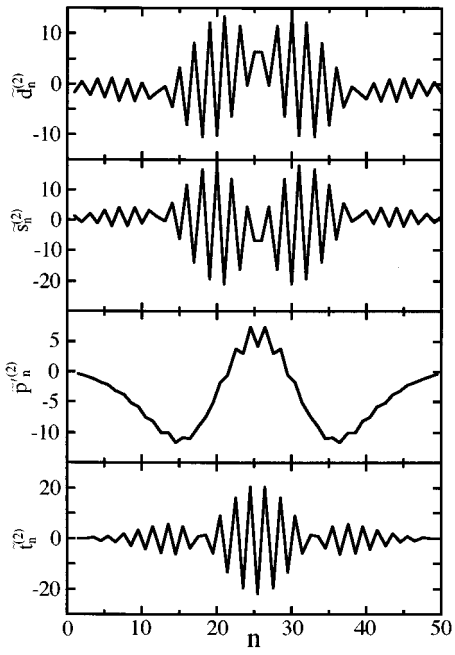

FIG. 17. The same physical quantities of Fig. 16, but to second order.

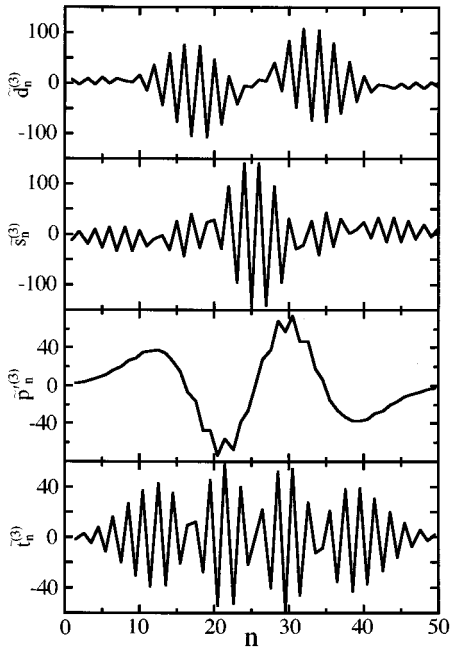

FIG. 18. The same physical quantities of Fig. 16, but to third order.

neutral soliton and a polaron are as follows. First, the half-filled regular chain has translational symmetry if the effects of chain boundaries are neglected. In contrast, these elementary excitations are characterized by the local deformation of four important physical quantities so that the symmetry is broken. Thus in the cases of a charged soliton, neutral soliton, and a polaron, there exist characteristic collective excitations of their translational oscillations. Second, a charged soliton and a polaron have a localized net charge and a neutral soliton and a polaron have localized net spin. Thus translational oscillation of a charged soliton or a polaron strongly couples with the external field and has very large contributions to their linear and nonlinear optics as shown in the previous section. Finally, the TDHF solution is symmetric with respect to spin exchange in the regular chain, but spin exchange symmetry is broken for a neutral soliton and a polaron. As a result, spin density and spin bond order fluctuations, which are not induced in the case of regular chain are induced by the external field in cases where the spin symmetry is broken. The following fluctuations induced by the external field dominate the response: collective translational oscillation and the coupled fluctuations of the amplitude of the charge density alternation and the soliton width in a charged soliton; polaronlike charge and spin bond order fluctuations and the coupled fluctuations of the amplitude of the spin density alternation and the soliton width in a neutral soliton; and, collective translational oscillation of a polaron and the coupled fluctuations of charge density, spin density and spin bond order alternation amplitudes and polaron width in a polaron. These essential physical aspects of the linear and nonlinear optical processes cannot be clearly described by the conventional sum over states method, which is based on the energy space picture. We have taken the electron–phonon coupling into account in calculating the geometry optimized HF solution, but lattice dynamics were neglected in the present calculations. Since the mass of a carbon atom is much heavier than that of an electron, the effect of lattice motions may usually be neglected for off resonant response. As shown in the previous section, translational oscillations of electronic structures of a charged soliton, a neutral soliton or a polaron play important roles in their linear and nonlinear response. Such electronic fluctuations strongly couple to the dynamical lattice motion of their translational motion. Moreover, in the case of polyacetylene, the soliton or polaron masses of their trnaslational motions are comparable to that of an electron.[1] Thus dynamical lattice motions will strongly affect the linear and nonlinear optics. Furthermore, quantum lattice fluctuations have been shown to significantly increase the off-resonant nonlinear optical susceptibilities.[35] This is an important subject for a future study. Note that it is straightforward to take the dynamics of lattice motions into account in our oscillator picture because this simply involves adding nuclear oscillators to the model.

ACKNOWLEDGMENTS

The support of the Air Force Office of Scientific Research and the National Science Foundation is gratefully acknowledged.

[1] A. J. Heeger, S. Kivelson, J. R. Schrieffer, and W. P. Su, Rev. Mod. Phys. **60**, 781 (1988), and references therein.
[2] *Conjugated Polymers and Related Materials,* edited by W. R. Salaneck, L. Lundstrom, and B. Banby (Oxford, New York 1993).
[3] J. L. Brédas, C. Adant, P. Tackx, A. Persoons, and B. M. Pierce, Chem. Rev. **94**, 243 (1994).
[4] H. Fukutome and M. Sasai, Prog. Theor. Phys. **69**, 373 (1983).
[5] M. Sasai and H. Fukutome, Prog. Theor. Phys. **70**, 1471 (1983).
[6] S. Etemad and Z. G. Soos, in *Spectroscopy of Advanced Materials,* edited by R. J. H. Clark and R. E. Hester (Wiley, New York, 1991), p. 87, and references therein.
[7] S. R. Marder, C. B. Gorman, F. Mayers, J. W. Perry, G. Bourhill, J. L. Brédas, and B. M. Pierce, Science **265**, 632 (1994).
[8] I. Ohmine and M. Karplus, J. Chem. Phys. **68**, 2298 (1978); K. Schulten, I. Ohmine, and M. Karplus, *ibid*. **64**, 4422 (1976); G. J. B. Hurst, M. Dupuis, and E. Clementi, *Nonlinear Optical Properties of Organic and polymeric Materials,* edited by D. J. Williams, Am. Chem. Soc. Symp. Ser. 233 (Am. Chem. Soc., Washington, D.C., 1983).
[9] B. E. Kohler, C. W. Spangler, and C. J. Westergfield, J. Chem. Phys. **94**, 908 (1991).
[10] I. D. W. Samuel, I. Ledoux, C. Dhenaut, J. Zyss, H. H. Fox, R. R. Schrock, and R. J Silbey, Science **265**, 1070 (1994).
[11] *Nonlinear Optical Properties of Organic and Polymeric Materials,* edited by D. J. Williams, Am. Chem. Soc. Symp. Ser. 233 (Am. Chem. Soc., Washington, D.C., 1983).
[12] *Nonlinear Optical Effects in Organic Polymers,* edited by J. Mrssier, F. Kajzar, P. N. Prasad, and D. R. Ulrich, NATO Advanced Study Institute, Ser. E, Vol. 162 (Kluwer Academic, Dordrecht, 1989).
[13] *Nonlinear Optical Properties of Organic Molecules and Crystals,* edited by D. S. Chemla and J. Zyss (Academic, New York, 1987).
[14] *Nonlinear Optical and Electroactive Polymers,* edited by P. N. Prasad and D. Ulrich (Plenum, New York, 1988).
[15] *Nonlinear Optical Properties of Polymers,* edited by A. J. Heeger, J. Orenstein, and D. R. Ulrich, Vol. 109 (MRS, Pittsburgh, 1988).
[16] B. J. Orr and J. F. Ward, Mol. Phys. **20**, 513 (1971).
[17] S. Mukamel and H. X. Wang, Phys. Rev. Lett. **69**, 65 (1992); H. X. Wang and S. Mukamel, J. Chem. Phys. **97**, 8019 (1992).
[18] S. Abe, M. Schreiber, W. P. Su, and J. Yu, Chem. Phys. Lett. **192**, 425 (1992); Phys. Rev. B **45**, 9432 (1992); Chem. Phys. **89**, 385 (1989).
[19] F. C. Spano and S. Mukamel, Phys. Rev. Lett. **66**, 1197 (1991); Phys. Rev. A **40**, 5783 (1989).
[20] S. Mukamel, *Nonlinear Optical Properties of Organic Molecules and Crystals,* Vol. 3, edited by J. Zyss (Academic, New York, 1992).

[21] A. F. Garito, J. R. Heflin, F. Y. Wong, and Q. Zamani-Khamiri, in *Organic Materials for Nonlinear Optics*, edited by R. A. Hann and D. Bloor, Special Publication No. 69 (Royal Soc. of Chem., London, 1988); J. R. Heflin, K. Y. Wong, Q. Zamani-Khamiri, and A. F. Garito, Phys. Rev. B **38**, 157 (1988); Mol. Crys. Liq. Crys. **160**, 37 (1988).
[22] A. Takahashi and S. Mukamel, J. Chem. Phys. **100**, 2366 (1994); S. Mukamel, A. Takahashi, H. X. Wang, and G. Chen, Science **266**, 250 (1994).
[23] P. Ring and P. Schuck, *The Nuclear Many-Body Problem* (Springer, New York, 1980).
[24] D. M. Mackie *et al.*, Phys. Rev. B **39**, 3442 (1989).
[25] J. R. Reimers and N. S. Hush, Chem. Phys. **176**, 407 (1993).
[26] J. Orenstein, in *Handbook of Conducting Polymaers*, Vol. 2, edited by T. A. Stokheim (Marcel Dekker, New York, 1986).
[27] H. Fukutome, J. Mol. Str. (Theochem) **188**, 337 (1989), and references therein.
[28] Z. G. Soos, in *Electroresponsive and Polymeric Systems*, Vol. 1, edited by T. A. Stokheim (Marcel Dekker, New York, 1988).
[29] D. Yaron and R. Silbey, Phys. Rev. B **16**, 776 (1978).
[30] E. R. Davidson, *Reduced Density Matrices in Quantum Density* (Academic, New York, 1976).
[31] R. McWeeny and B. T. Sutcliffe, *Methods of Molecular Quantum Mechanics* (Academic, New York, 1976).
[32] P. O. Löwdin, Phys. Rev. **97**, 1474 (1955); A Reed, L. A. Curtiss, and F. Weinhold, Chem. Rev. **88**, 899 (1988).
[33] A. Stahl and I. Balslev, *Electrodynamics of the Semiconductor Band Edge* (Springer, Berlin, 1987).
[34] Y. Shimoi and S. Abe, Phys. Rev. B **50**, 14 781 (1994).
[35] T. W. Hagler and A. J. Heeger, Chem. Phys. Lett. **189**, 333 (1992).